THE ASTROPHYSICAL JOURNAL, 446:L5–L9, 1995 June 10

INFRARED CORONAL LINE WIDTHS IN TYPE 1 SEYFERT GALAXIES[1]

E. GIANNUZZO[2]
Università degli Studi di Bologna, via Zamboni 33, I-40126, Bologna, Italy
G. H. RIEKE
Steward Observatory and Department of Planetary Sciences, University of Arizona, Tucson, AZ 85721
AND
M. J. RIEKE
Steward Observatory, University of Arizona, Tucson, AZ 85721
Received 1994 November 18; accepted 1995 March 27

ABSTRACT

We present high-resolution observations of six Seyfert 1 galaxies in the 2 μm region. We detected the [Si VI] 1.96 μm coronal line in all the galaxies and analyzed its profile, finding it to be variable in width from object to object, from very narrow profiles (FWHM $\sim$ 300 km s^{-1}) to profiles approaching the width of the broad lines. The coronal region seems to be placed differently in different galaxies, and in some cases the infrared coronal lines are useful as a probe of the structure of the broad-line region.

Subject headings: galaxies: active — galaxies: Seyfert

1. INTRODUCTION

The origin of the so-called coronal lines in active galactic nuclei (AGNs) is still an open and much-debated question, even many years after the discovery of the optical iron lines, among which are high-ionization ($h\nu_{ion} \gtrsim 100$ eV) forbidden lines of [Fe VII], [Fe X], [Fe XI], and [Fe XIV]. The ionization mechanisms suggested so far for the coronal lines are collisional ionization of a hot ($T \sim 10^6$ K) gas (Oke & Sargent 1968; Nussbaumer & Osterbrock 1970), photionization of the diffuse interstellar gas by the central source (Osterbrock 1969; Nussbaumer & Osterbrock 1970; Grandi 1978; Korista & Ferland 1989), or a combination of shocks and photoionization (Viegas-Aldrovandi & Contini 1989). For example, while Korista & Ferland (1989) modeled a low-density emitting gas located out of the narrow-line region (NLR), Spinoglio & Malkan (1992) explored the possibility of a dense, highly ionized medium just outside the broad-line region (BLR).

Besides the optical lines, coronal lines have been detected between 1.5 and 4 μm in several novae and high-excitation planetary nebulae. Oliva & Moorwood (1990) also reported the observation of the [Si VI] 1.96 μm and [Si VII] 2.48 μm lines in the Seyfert 2 galaxy NGC 1068, followed by the detection of these and other IR coronal lines in the Circinus (Seyfert 2) galaxy (Oliva et al. 1994); Marconi et al. (1994) have recently conducted a survey for [Si VI] 1.96 μm emission in a sample of southern active, starburst, and *IRAS* ultraluminous galaxies. These works imply that the infrared coronal lines can perhaps be used to help determine the excitation mechanism and the location of the coronal line region (CLR). In particular, these lines should be useful both because of their relative immunity to interstellar reddening and also because of the greatly expanded list of lines at high critical densities they make accessible beyond those represented by the optical lines.

For these reasons, we observed a sample of six Seyfert 1 galaxies in the 2 μm region to measure the intensities and profiles of coronal lines of [Si VI] at 1.96 μm and of [Ca VIII] at 2.32 μm, so we could compare their properties with those of the other infrared and optical lines we observed almost simultaneously. The analysis of the line profiles gives us information on the gas kinematics and density in the line-emitting region. In particular, the [Si VI] line is potentially very interesting because its critical density, $\sim 6 \times 10^8$ cm^{-3} (Greenhouse et al. 1993 and references therein), allows it to probe gas to densities approaching the lowest in the BLR, so it can be used to discriminate among a number of the possibilities listed above for the nature of the coronal region.

2. NEW OBSERVATIONS

The IR observations were obtained with FSPEC (Williams et al. 1993) on the Multiple Mirror Telescope. This instrument is a long-slit spectrometer using a 256 × 256 NICMOS3 HgCdTe detector array. As used on the MMT, each pixel projects to 0".4, and the slit is 30" long by 1" wide. The nuclei of the galaxies were placed on the slit using an off-the-slit visible light acquisition TV, and spectra were obtained moving the telescope between integrations so the source was observed at four locations along the slit. Most of the observations used a 600 groove mm^{-1} grating, giving a per pixel resolution of $\sim$40 km s^{-1} at the long-wavelength end of the K atmospheric window and $\sim$50 km s^{-1} at the short end. Measurements of solar-type standard stars close on the sky to the Seyfert galaxies were closely interspersed with the galaxy measurements to allow accurate correction for terrestrial atmospheric absorptions, which are strong at the rest wavelength of the [Si VI] line, and observations were made on relatively dry nights. These strategies have resulted in an excellent correction of the spectra for water vapor features, which would otherwise have made it impossible to detect the [Si VI] line reliably. Figure 1 compares the spectra of a galaxy and reference star for the most difficult case we observed (because of its small redshift). Note the excellent agreement away from the indicated emission lines, and that the atmospheric transmission in the spectral range of

[1] Observations reported in this paper were obtained with the Multiple Mirror Telescope, which is operated jointly by the Smithsonian Astrophysical Observatory and the University of Arizona.
[2] Visiting Steward Observatory.

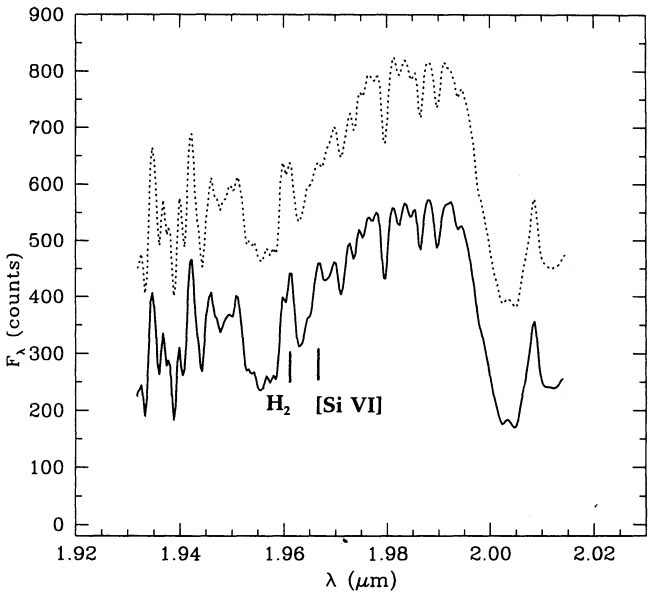

FIG. 1.—Raw spectra for NGC 4051 (*solid line*) and its comparison star, HR 4572 (*dotted line* [*offset for clarity*]). The H_2 (1, 0) $S(3)$ and [Si VI] lines are marked in the galaxy spectrum.

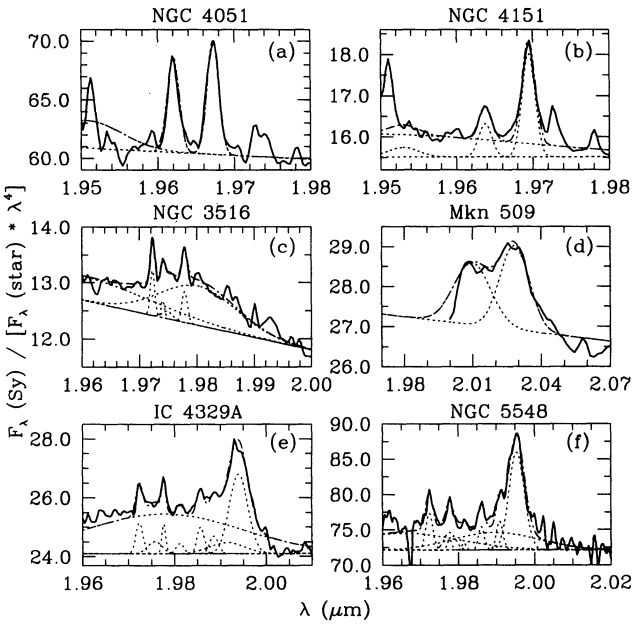

FIG. 2.—[Si VI] line region in the observed galaxies: the measured spectra (*solid lines*), the Gaussian fits with which we deblended them (*dashed lines*), and the total fitted spectra (*dot-dashed lines*) are plotted. The weak unresolved lines are artifacts of absorptions in the comparison stars. Spectra are arbitrarily normalized.

interest is $\geq 60\%$. An approximate calibration of the data was obtained by assuming standard colors for the comparison star. However, given the narrow slit, we do not expect this value to be more accurate than a factor of 1.5; the emphasis in this paper is on the line profiles and relative strengths.

The optical data were taken with a Boller & Chivens spectrograph coupled with a 1200 × 800 CCD camera, at the 90 inch (2.3 m) Steward telescope on Kitt Peak. We used different 600 groove mm^{-1} gratings in different observing nights, respectively centered at 3565, 3658, and 4458 Å, the Hβ region being covered by all of them. The spectra were obtained with a standard procedure, and our objects are bright enough to reach a high signal-to-noise ratio (S/N) easily.

3. DATA REDUCTION

The reduction of the optical observations was performed with the standard IRAF reduction tasks. We used averaged dark frames to correct for offset and dark-current terms, and flat-field frames to eliminate pixel response effects. The sky subtraction was automatically made while extracting the one-dimensional spectra from the images, and a He-Ar lamp was used for wavelength calibration.

The IR data reduction was performed using both IRAF reduction tasks and particular codes and tasks written for FSPEC data. The first step is background subtraction, realized by subtracting from each frame a combination of frames taken at adjacent positions on the slit (this step also removes offset and dark-current terms). The spectra are then corrected for the geometric distortions in the spectrograph optics. We corrected the spectra for response nonuniformities with a flat-field frame generated from dome flats from which a dark-current frame has been subtracted. A bad-pixel mask is used to mark bad pixels and remove them in further processing. A one-dimensional spectrum can then be extracted. Atmospheric absorptions are corrected by dividing the galaxy spectrum by a combination of the spectra of the reference star obtained before and after the galaxy observations (typically over a period of less than 10 minutes). The spectrum is wavelength-calibrated with OH airglow lines in the sky spectrum (Oliva & Origlia 1992). In the case of the high-resolution spectra taken at 2.34 μm for NGC 3516, we used a Ne-Kr lamp for wavelength calibration. Finally, we divided each spectrum by a λ^4 curve, to correct for the slope introduced by the star continuum. The region around the [Si VI] line is shown for each galaxy in Figure 2.

We chose the reference star so that its spectrum has few absorption features (G or F spectral type). Nonetheless, some artifacts from the star must be removed from the spectrum of the galaxy. We could easily fit and remove the strong Brγ absorption in the stellar spectra, but weaker features such as Brδ and several Si, Ca, C, and Fe lines are left and appear in emission in our final spectra. We identified these lines using high-resolution solar spectra and fitted them in the same way we performed the fit to the nuclear lines, so that no contamination from these features could enter in our evaluation of the physical parameters of the lines of interest. We left the feature strengths as free parameters because such information is not yet available for an adequate network of stars similar to the ones we used. These stellar features appear as weak, unresolved emission features in the fits of Figure 2.

4. ANALYSIS

The identification of each detected line from the galaxies and the estimate of its position, width, and strength were conducted on the fully reduced spectra through standard IRAF Gaussian line-fitting tasks. The [Si VI] 1.96 μm line is clearly detected in every object. The coronal line is close to (and sometimes blended with) both the hydrogen Brδ emission feature and the (1, 0) $S(3)$ H_2 line, so to analyze the [Si VI] feature we needed first to evaluate the strength and shape of the H I line. Therefore, we fitted the stronger Brγ emission line, and assumed the

TABLE 1

EMISSION-LINE PARAMETERS

Line	NGC 3516 (Brγ)[a]	NGC 4051 (Brγb)	NGC 4151 (Brγb)	IC 4329A (Brγb)	NGC 5548 (Hβ)[b]	Mkn 509 (Brγ)
H_2 (1, 0) $S(3)$ (1.9570)[b]	1.9578(5)[c]	1.957(3)	1.9572(8)	1.957(1)	1.9573(9)	...
	304[d]	275	305	332	301	...
	0.021[e]	0.26	0.11	0.056	0.11	...
[Si VI] (1.9629)	1.963(3)	1.9624(5)	1.9630(5)	1.962(1)	1.9617(7)	1.962(9)
	2350	274	305	707	707	2220
	0.95	0.31	0.34	0.54	0.94	1.3
H recombination (2.1655, 0.4861)	2.1619(5)	2.1652(5)	2.160(5)	2.1704(8)	0.489(4)	2.167(5)
	4540	1610	7480	5990	3940	2890
	1.8	0.62	4.0	3.4	34	2.2
[Ca VIII] (2.3214)	~2.321(1)	...	~2.319(3)	...	...	...
	~1280	...	~1220	...	...	...
	~0.21	...	~0.20	...	...	...
F_λ[f]	0.5	0.35	1.2	1.0	0.5	0.23
z	0.00868	0.00242	0.00332	0.01605	0.01718	0.03400

[a] Recombination line for which properties are tabulated.
[b] Expected rest wavelength in microns.
[c] Measured wavelength in microns, corrected to rest wavelength; the uncertainty in the last digit is given in parentheses.
[d] Measured FWHM in km s^{-1}.
[e] Equivalent width in nanometers.
[f] Flux density at 2.0 μm, in units of 10^{-16} W m^{-2} nm^{-1}.

same redshift and profile for the Brδ feature, and a Brγ/Brδ ratio of 1.51 (Osterbrock 1989). In one case (NGC 5548) we could not observe the Brγ region, so we used the optical Hβ line to determine the Brδ profile, and evaluated the line strength according to the best fit. To test this latter procedure, we compared the Brγ and Hβ profiles in the four galaxies for which both lines were observed, finding that, with only one exception, the Brγ components are usually broader or approximately (within 10%) of the same width as the Hβ components. We also used the Hβ line in the case of IC 4329A to help separate the various components of Brγ, since its broad component is larger than the spectral range covered by our grating setting in the high-resolution mode. Where the hydrogen recombination lines had complex profiles, we achieved approximate fits to Brδ by using more than one Gaussian (NGC 4151, IC 4329, and NGC 5548).

The results of the fit of the silicon coronal line and the H_2 (1, 0) $S(3)$ line at 1.957 μm are reported in Table 1, where the FWHMs and the equivalent widths of the lines are indicated, together with the same parameters for the hydrogen line we used to constrain the Brδ profile. We indicate in parentheses which line we used to determine the hydrogen line profile and, when necessary, for which component of the line we measured the reported parameters (usually the main, broad component).

The coronal [Ca VIII] 2.32 μm feature lies in a spectral region where normal galaxies are dominated by deep CO $\Delta v = 2$ absorption bands produced in the atmospheres of late-type stars, and the line lies almost at the bandhead of one of these features. We observed the 2 μm region at low resolution in Mrk 509, NGC 4051, and NGC 4151: in the first two objects the line was not intense enough to give a certain detection, while in the case of NGC 4151 it is quite intense compared with the absorption bands, and is considerably broader than the silicon line (as also found by Thompson 1994). The fit is shown in Figure 3. We also obtained a high-resolution observation in this spectral range for NGC 3516. To analyze this spectrum, we applied a Gaussian broadening function to an appropriately redshifted late-type stellar spectrum to produce a synthetic, velocity-broadened spectrum of the stars in the galaxy. We normalized the synthetic spectrum and adjusted the broadening to minimize the difference between it and the spectrum of the galaxy, as shown in Figure 4*a*. This method allowed a tentative detection of the calcium coronal line and a rough estimate of its strength and width (see Fig. 4*b*). In this case the line appears to be narrower than the silicon line, but the uncertainties in the detection method lead us to consider the indicated FWHM to be a lower limit because of possible errors in the placement of the continuum level.

The molecular hydrogen line at 1.957 μm, which we detected in most galaxies, has a narrow profile, in accordance with most of the objects in the Marconi et al. (1994) survey. The presence of this line is common in starburst galaxies and AGNs, but its origin and excitation mechanism are still unclear. The main processes suggested so far are X-ray heating, shock heating,

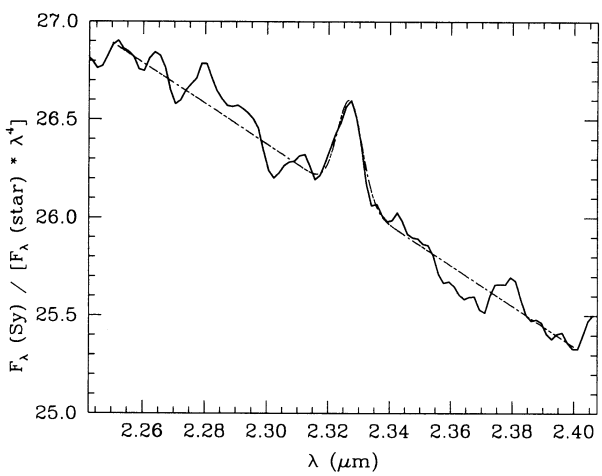

FIG. 3.—[Ca VIII] 2.32 μm line in NGC 4151: notation is as in Fig. 2

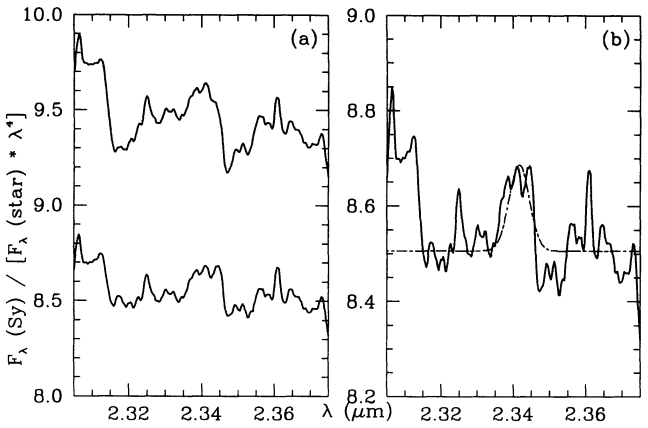

FIG. 4.—[Ca VIII] 2.32 μm line in NGC 3516: (*a*) comparison of the original spectrum (*above*) and the one obtained by subtracting a synthetic galactic spectrum (*below*); (*b*) fit of the coronal line: notation is as in Fig. 2.

UV pumping, or a mixture of more than one mechanism (Moorwood 1989; Kawara, Nishida, & Gregory 1990).

5. DISCUSSION

The [Si VI] line shows three distinct types of behavior in the six galaxies we have observed. This range of behavior confirms and extends the range observed in optical studies of the iron coronal lines and probably indicates that the coronal line region occupies different regions in different Seyfert galaxies. We discuss these three cases below.

In NGC 4051 and NGC 4151 the [Si VI] line has approximately the same width as the H_2 1.957 μm line, and is somewhat narrower than the narrow components of the hydrogen lines (Hβ, Hγ, Hε, Brγ), He II λ4685, and the forbidden [O III], [O II], [Ne III] optical features. Given the high critical density for the [Si VI] line, this behavior confirms the conclusions of De Robertis & Osterbrock (1984) for these two galaxies that there is no correlation between critical density and forbidden line width. The observations are consistent with models similar to that of Korista & Ferland (1989), where the CLR might be associated with the quiescent interstellar medium (ISM) of the galaxy photoionized by the nuclear UV source. In these models, the excited region must be restricted in angular extent to be consistent with the size observed for the CLR. This behavior could also be reconciled with the CLR lying in a NLR of various specific structures, such as some relatively high velocity gas not being exposed to the hardest nuclear radiation.

In Mrk 509 and NGC 3516 the [Si VI] line is much broader than typical narrow lines and, particularly for Mrk 509, approaches the width of lines from the BLR. This profile is consistent with the general trend for forbidden line widths to be correlated with critical density (e.g., De Robertis & Osterbrock 1984, 1986), a trend that seems to hold specifically for Mrk 509, for which Penston et al. (1984) report a width of 1050 km s^{-1} for the high critical density line of [Fe X]. Given the widths of the [Si VI] lines, in these galaxies the coronal emission would appear to originate in a region intermediate between the BLR and the NLR, or in the lowest density portions of the BLR. To first order, we can take the relative strengths of [Si VI] and Brγ to be in proportion to their equivalent widths, given the small wavelength interval separating them. We find that the [Si VI] line is only an order of magnitude weaker (relative to Brγ) in these galaxies than for the calculations of Korista & Ferland (1989) and of Spinoglio & Malkan (1992). This observation places a lower limit on the proportion of the BLR with density below the critical density for [Si VI], i.e., 6×10^8 cm^{-3}, indicating that it is a substantial fraction of the BLR.

NGC 5548 and IC 4329A are an intermediate case, where the [Si VI] has a width similar to (or slightly larger than) the widths of the "standard" narrow (permitted and forbidden) lines (in both objects we used Hβ to constrain the Brackett lines [see § 4], so the IR hydrogen lines are not useful in the comparison). We could therefore suppose the Si^{+5}-emitting gas to lie at or slightly inside the NLR, and possibly to be in pressure equilibrium with the narrow-line clouds.

Because most of the infrared coronal line detections in the literature (Oliva & Moorwood 1990; Ward et al. 1991; Oliva et al. 1994; Marconi et al. 1994) apply to Seyfert 2 galaxies where the BLR is likely to be very heavily obscured (Antonucci & Miller 1985), it is difficult to tell whether these galaxies fall into the same categories discussed above. In the Marconi et al. survey there are eight total Seyfert [Si VI] detections listed (some of them were known previously): five of these are Seyfert 2's and two of those are very weak detections (3 σ). There are three Seyfert 1's with detected [Si VI] lines, one of which (IC 4329A) overlaps with our sample, and the observed line profiles are in good agreement (width comparable to those in the NLR). The other two objects both present quite good detections belonging to the "very narrow" line category. So if we consider all the [Si VI] detections obtained so far in Seyfert 1 galaxies, we find that, out of eight objects, four belong to the "very narrow" category, two to the "narrow" one, and two to the "intermediate" (i.e., between BLR and NLR) one. As regards the detections in Seyfert 2 objects, while in NGC 1068 and Cygnus A the [Si VI] line is broader than the other emission lines, and therefore probably belongs to the "intermediate" category, the Circinus galaxy and the newly detected objects in the Marconi et al. survey (four galaxies in total) all present "very narrow" silicon features.

6. CONCLUSIONS

We report high-resolution observations of the coronal line [Si VI] 1.96 μm and other infrared lines in six Seyfert 1 galaxies. In most objects this is the first detection of the silicon coronal line. We have analyzed the line profile, in comparison with the other observed features and with published data. The infrared coronal lines present a variety of widths from galaxy to galaxy, from very narrow ones (~300 km s^{-1}) to widths comparable to the classical NLR profiles (~500–1000 km s^{-1}) and ranging to profiles approaching the broad lines in width. This behavior suggests that the coronal line region is placed differently in different galaxies, ranging respectively from excited interstellar medium to the low-density zones of the BLR. As a result, these lines represent a promising tool to investigate the structure of the emission-line regions around AGNs.

We thank J. Liebert for help with the optical observations and L. Shier and C. Engelbracht for assistance in data reduction and analysis. J. Shields provided helpful comments on the manuscript. E. G. appreciates the financial support of the Rotary International through a Rotary Foundation grant. This work was also supported by the National Science Foundation.

REFERENCES

Antonucci, R. R. J., & Miller, J. S. 1985, ApJ, 297, 621
De Robertis, M. M., & Osterbrock, D. E. 1984, ApJ, 286, 171
———. 1986, ApJ, 301, 727
Grandi, S. A. 1978, ApJ, 221, 501
Greenhouse, M. A., Feldman, U., Smith, H. A., Klapisch, M., Bhatia, A. K., & Bar-Shalom, A. 1993, ApJS, 88, 23
Kawara, K., Nishida, M., & Gregory, B. 1990, ApJ, 352, 433
Korista, K. T., & Ferland, G. J. 1989, 343, 678
Marconi, A., Moorwood, A. F. M., Salvati, M., & Oliva, E. 1994, A&A, 291, 18
Moorwood, A. F. M. 1989, in Proc. 22d ESLAB Symp. on Infrared Spectroscopy in Astronomy, ed. A. C. H. Glasse, M. F. Kessler, & R. Gonzales-Riesta (ESA SP-290; Paris: ESA), 431
Nussbaumer, H., & Osterbrock, D. E. 1970, ApJ, 161, 811
Oke, J. B., & Sargent, W. L. W. 1968, ApJ, 151, 807
Oliva, E., & Moorwood, A. F. M. 1990, ApJ, 348, L5
Oliva, E., & Origlia, L. 1992, A&A, 254, 466
Oliva, E., Salvati, M., Moorwood, A. F. M., & Marconi, A. 1994, A&A, 288, 457
Osterbrock, D. E. 1969, Astrophys. Lett., 4, 57
———. 1989, Astrophysics of Gaseous Nebulae and Active Galactic Nuclei (Mill Valley: University Science Books)
Penston, M. V., Fosbury, R. A. E., Boksenberg, A., Ward, M. J., & Wilson, A. S. 1984, MNRAS, 208, 347
Spinoglio, L., & Malkan, M. A. 1992, ApJ, 399, 504
Thompson, R. I. 1994, ApJ, in press
Viegas-Aldrovandi, S. M., & Contini, M. 1989, A&A, 215, 253
Ward, M. J., Blanco, P. R., Wilson, A. S., & Nishida, M. 1991, ApJ, 382, 115
Williams, D. M., Thompson, C. L., Rieke, G. H., & Montgomery, E. F. 1993, Proc. SPIE, 1946, 482